Molecular Dynamics of Alamethicin Transmembrane Channels from Open-Channel Current Noise Analysis

Don-On Daniel Mak* and Watt W. Webb†
*Physics Department, †School of Applied and Engineering Physics, Cornell University, Ithaca, New York 14853 USA

ABSTRACT Conductance noise measurement of the open states of alamethicin transmemberane channels reveals excess noise attributable to cooperative low-frequency molecular dynamics that can generate fluctuations ≈1 Å rms in the effective channel pore radius. Single-channel currents through both persistent and nonpersistent channels with multiple conductance states formed by purified polypeptide alamethicin in artificial phospholipid bilayers isolated onto micropipettes with gigaohm seals were recorded using a voltage-clamp technique with low background noise (rms noise <3 pA up to 20 kHz). Current noise power spectra between 100 Hz and 20 kHz of each open channel state showed little frequency dependence. Noise from undetected conductance state transitions was insignificant. Johnson and shot noises were evaluated. Current noise caused by electrolyte concentration fluctuation via diffusion was isolated by its dependence on buffer concentration. After removing these contributions, significant current noise remains in all persistent channel states and increases in higher conductance states. In nonpersistent channels, remaining noise occurs primarily in the lowest two states. These fluctuations of channel conductance are attributed to thermal oscillations of the channel molecular conformation and are modeled as a Langevin translational oscillation of alamethicin molecules moving radially from the channel pore, damped mostly by lipid bilayer viscosity.

GLOSSARY

List of relevant symbols used in this paper and their definitions:

i_n^{ch} Amplitude of current passing through the alamethicin channel in conductance state n.
Λ_n Conductance value of the alamethicin channel in state n.
$\langle S_i(f)\rangle_n$ Power spectral density (PSD) of current noise averaged over all the intervals during which the alamethicin channel observed is in conductance state n in an experimental current record.
$S_i(f)_n^{ch}$ PSD of current noise due only to the alamethicin channel in conductance state n with the instrumental background noise removed = $\langle S_i(f)\rangle_n - \langle S_i(f)\rangle_o$.
$[S_i]_n^{ch}$ Characteristic PSD value of alamethicin channel current noise within the observed frequency range = $S_i(f)_n^{ch}$ averaged over all f between 100 Hz and 20 kHz.
$[S_i]_n^{s}$ Calculated current PSD value for shot noise in the alamethicin channel in conductance state n.
$[S_v]_n^{s}$ Calculated voltage PSD value for shot noise in the alamethicin channel in conductance state n.
$[S_v]_n^{J}$ Calculated voltage PSD value for Johnson noise in the spreading resistance around the alamethicin channel in state n.
$[S_i]_n^{J\&s}$ Calculated current PSD value for combined shot and Johnson noises associated with the alamethicin channel in state n.
$[\Delta S_i]_n$ $[S_i]_n^{ch} - [S_i]_n^{J\&s}$
S_n^{ion} Dimension-free normalized PSD due to ion concentration fluctuation in and around the alamethicin channel in conductance state n = part of $[\Delta S_i]_n/(i_n^{ch})^2$ that has buffer electrolyte concentration dependence.
S_n^{mol} Dimension-free normalized PSD attributed to thermal molecular motion in the alamethicin channel in conductance state n = part of $[\Delta S_i]_n/(i_n^{ch})^2$ that is independent of buffer electrolyte concentration.
r_n^{eq} Equivalent radius of the alamethicin channel in conductance state n = radius of a circular hole in an infinite bilayer that has the same spreading resistance as the channel.
r_n^{max} Maximum radius of an ion that can pass through the alamethicin channel according to the modified barrel-stave model.

INTRODUCTION

Protein conformation fluctuations and librations are known to occur over a wide range of time scales (sub-picoseconds to seconds and beyond) and amplitude (from picometers to nanometers) (Karplus and McCammon, 1983). Such libration is essential to many protein functions like enzyme activity (Huber, 1979; Chou and Chen, 1977; Chou et al., 1981), ligand-induced response (Frauenfelder and Young, 1986; Schlessinger, 1986), and protein channel gating (Hille, 1984; Millhauser et al., 1988). Many of these vital functions occur in intrinsic proteins bound in a lipid membrane. However, application of experimental methods like nuclear magnetic resonance (Gurd and Rothgeb, 1979) and x-ray diffraction (Petsko and Ringe, 1984) to probe the conformation of a membrane-bound protein in its native environment is hampered by the limited quantity of functional membrane-bound proteins that can be isolated inside a bilayer. The complexity of the bilayer environment and the long time scale (microseconds to milliseconds) involved in many of the protein activities (like channel gating) make theoretical studies like molecular dynamics simulation (Karplus and McCammon, 1983; Karplus, 1987; Karplus and Petsko, 1990) extremely difficult.

Received for publication 6 February 1995 and in final form 7 September 1995.

Address reprint requests to Dr. Don-On Daniel Mak, Department of Physiology, University of Pennsylvania, Stellar-Chance Laboratories, Rm 313B, 422 Curie Blvd., Philadelphia, PA 19104 USA Tel: 215-898-0468; Fax: 215-573-8590

0006-3495/95/12/2337/13 $2.00

With the development of "patch-clamp" technique (Hamill et al., 1981; Cahalan and Neher, 1992), it is possible to make high-quality, low-background-noise records (Sigworth, 1985) of ion currents passing through individual protein channels in cell membranes or artificial lipid bilayers isolated at the tips of micropipettes (radius ~1 μm; Sakmann and Neher, 1983) with stable, gigaohm seals under constant applied voltage for extensive periods of time (minutes, even hours). Because the magnitude of the current passing through the channels is directly affected by the structure of the channels, fluctuation in the conformation of the channel will result in channel current fluctuation (Stevens, 1972). Therefore, noise in the open-channel current offers a valuable probe into molecular libration and conformational fluctuation in channel proteins in a membrane environment at the frequency range between 100 Hz to 100 kHz (Sigworth, 1985, 1986). This can give us more insight into the multitude of interactions that govern the behavior of membrane-bound proteins.

Alamethicin is a well-studied polypeptide containing 20 amino acid residues capable of forming well-defined, voltage-dependent channels in many biological membranes and synthetic lipid bilayers (Latorre and Alvarez, 1981; Sansom, 1991; Woolley and Wallace, 1992). It can, under a wide range of experimental conditions, form stable channels that last for long periods so that many samples of current noise spectra can be obtained for analysis. Its simple, well-established primary structure (Rinehart et al., 1977) and the many studies done on its secondary structures in various environments (Sansom, 1991; Woolley and Wallace, 1992) allow simple models to be constructed to explain the molecular origin of the observed channel current noise.

In our preceding paper (Mak and Webb, 1995), the electrical and kinetic properties of two classes of alamethicin channels were described. The *persistent* channels last a long time (minutes to hours) and appear at a low applied potential (~30 mV). The *nonpersistent* channels are induced by pulsing the applied potential to a higher level (~120 mV) and last a short time (<1 min). Each of the two classes of channels has a distinctive set of conductance states. Our molecular models suggested that whereas all the alamethicin monomers in the persistent channel aggregate are aligned parallel to the applied electric field as described by the "barrel-stave" model (Baumann and Mueller, 1974), one of the alamethicin monomers in the nonpersistent channel aggregate is oriented antiparallel to the external electric field and the rest of the monomers.

In this paper we report a detailed analysis of the current noise observed in persistent and nonpersistent alamethicin channels. Contributions to open-channel current noise from background noise sources (undetected brief conductance state transitions, shot noise, Johnson noise, and buffer concentration fluctuation via random ion diffusion) were evaluated and removed from the observed open-channel current noise. The remaining current noise is attributed to molecular thermal fluctuations that affect the structure and therefore the conductance of the channel. The channel molecular oscillation was modeled by a Langevin translational oscillation of alamethicin monomers moving radially from the channel pore. An estimate of the amplitude of the thermal molecular oscillation was made, assuming that the oscillation is mainly damped by lipid bilayer viscosity.

A list of relevant symbols used in this paper and their definitions is included in the Glossary for easy reference.

MATERIALS AND METHODS

Alamethicin purchased from Sigma Chemical Co. (St. Louis, MO) was purified by high-performance liquid chromatography following the procedures used by Balasubramanian et al. (1981) to obtain alamethicin R_f50 samples (Archer et al., 1991) used in the experiment. The alamethicin R_f50 molecule has the primary sequence (Martin and Williams, 1975; Archer et al., 1991): Ac-Aib-Pro-Aib-Ala-Aib^5-Ala-Gln-Aib-Val-Aib^{10}-Gly-Leu-Aib-Pro-Val^{15}-Aib-Aib-Gln-Gln-Phol^{20}, where Aib and Phol stand for α-aminoisobuteric acid and L-phenylalaninol, respectively. It is electrically neutral at pH 7.

A solvent-free tip-dip technique was used to obtain stable gigaohm seals on the tips of micropipettes for the patch-clamp experiments (Mak and Webb, 1995), using a 1:1 mixture of synthetic dioleoyl phosphatidylethanolamine (DOPE) and dioleoyl phosphatidylserine (DOPS) from Avanti Polar Lipids, Inc. (Alabaster, AL). Experiments using 2:2:1 mixture of DOPE:DOPS:cholesterol (cholesterol from Nu Chek Prep Inc., Elysian, MN), or azolectin (Sigma Chemical Co.) yielded qualitatively similar channel current noise measurements. Buffer solution containing 5 mM $CaCl_2$, 1 mM $MgCl_2$, 30 mM HEPES at pH 7 and a variable NaCl concentration between 0.33 and 2.0 M was used. The same buffer was used on both sides of the lipid bilayer in all experiments. Alamethicin (0.2 μg/ml) was used in the pipette buffer. To decrease the frequency of transitions between the conductance states of the alamethicin channels, the bath buffer solution was cooled (Boheim, 1974; Gordon and Haydon, 1976; Boheim and Kolb, 1978) to 7.0 ± 0.2°C with a Peltier cooling stage (OPMI-2; Medical Systems Corp., Greenvale, NY).

Single-channel alamethicin current at applied potential between −68 and 80 mV was amplified by a patch-clamp amplifier (3900A with headstage 3901; Dagan Corp., Minneapolis, MN). The output was digitized at 94.4 kHz and filtered with a 4-pole Bessel filter at 37.0 kHz by a pulse code modulator (VR-10; Instrutech Corp., Mineola, NY). Conductance state transitions in a current record were detected by the computer program described in our preceding paper (Mak and Webb, 1995). Continuous intervals containing 2048 data points (21.7 ms) were automatically selected by the data analysis program if no conductance state transition was detected in them. For each selected interval, the fluctuation of the current about the mean current level in that interval was Fourier transformed with Hanning windowing (Press et al., 1987a) to obtain the power spectral density (PSD) $S_i(f)$ of the current noise in that interval. All noise power spectra obtained when the channel was in conductance state n were averaged to give the mean power spectrum $\langle S_i(f)\rangle_n$ for that state.

A typical single-channel record examined consists of 2 to 6 min of data records during which the channel was active. Depending on the rate of conductance state transitions, such a data record gives about 3,000–10,000 acceptable samples of the current noise power spectra in various conductance states. For nonpersistent channels, the current record examined usually consists of several (two to five) bursts of open channel activity, each generated by an inducing pulse in the applied potential.

The frequency response of the data acquisition system was checked by measuring the Johnson noise (Nyquist, 1928) in a known resistance. The current noise power spectrum between 100 Hz and 20 kHz obtained as described above deviated from the theoretical Johnson noise value by less than the experimental error limits.

To estimate the contribution of undetected rapid conductance state transitions to the measured channel current noise, the dwell-time distribution histograms for "up pulses" in which the channel goes from conductance state $(n - 1)$ to state n back to state $(n - 1)$ and "down pulses" with

state $(n + 1)$ to state n back to state $(n + 1)$ transitions were constructed for all persistent and nonpersistent channel conductance states n (Opsahl, 1993). The visits of the channel to state n were first sorted into four different categories: those involving transition sequences $(n - 1) \rightarrow n \rightarrow (n - 1)$, $(n + 1) \rightarrow n \rightarrow (n + 1)$, $(n - 1) \rightarrow n \rightarrow (n + 1)$, and $(n + 1) \rightarrow n \rightarrow (n - 1)$. Then visits in each category were sorted according to the time the channel spent in state n (Sigworth and Sine, 1987) to generate the dwell-time histogram.

EXPERIMENTAL CURRENT NOISE POWER SPECTRA

In our preceding paper (Mak and Webb, 1995), the channels formed by alamethicin R_f50 can be separated by their kinetic properties and conductance values into two distinct classes: the persistent channels that stay open for extended periods without closing, and the nonpersistent channels that only open in relatively short, brief pulses induced by a higher applied potential. Each class of channels has a different set of conductance values for the various conductance states. The open-channel current noise levels found in the two different classes of channels are also markedly different.

Fig. 1 shows the mean current noise power spectra $\langle S_i(f)\rangle_n$ of a typical persistent channel in various conductance states. The 0th conductance state is the closed channel, and its noise spectrum $\langle S_i(f)\rangle_o$ is due to noise not associated with the channel like noise from the lipid bilayer and instrumentation (Sigworth, 1983). In most experiments with stable lipid bilayers, $\langle S_i(f)\rangle_o$ is identical to the background noise spectrum for the bare bilayer before any channel activity appeared. The rise in the background noise at higher frequencies is probably due to thermal current noise in the field-effect transistor (FET) used in the patch-clamp amplifier (van der Ziel, 1970; Sigworth, 1983) and is found in all experiments using similar patch-clamp instrumentation (Sigworth, 1985; Sigworth et al., 1987). Because of the smaller membrane capacitance in our experiments, the background noise at higher frequencies (1–20 kHz) from our solvent-free lipid bilayers is substantially lower than that from black lipid membranes (Bezrukov and Vodyanoy, 1991; Bezrukov et al., 1994) formed by the Montal-Mueller method (Montal and Mueller, 1972), allowing a wider frequency range to be examined. The 0th state noise spectrum was subtracted from the open-channel current noise spectra to obtain the current noise spectra due to the channel alone, $S_i(f)_n^{ch} = \langle S_i(f)\rangle_n - \langle S_i(f)\rangle_o$ (Sigworth, 1985).

Because of the rise in instrumental background noise at higher frequencies (Fig. 1), the ratio between channel noise and background noise is too small for detailed inspection beyond 20 kHz. Because the shortest mean dwell time for an alamethicin channel conductance state (persistent or nonpersistent) is ~0.1 s (Mak and Webb, 1995), the low-frequency limit of the power spectra was chosen to be 100 Hz to give a reasonably large number of spectra to be averaged for each conductance state. Between 100 Hz and 20 kHz, the channel current noise power spectral density (PSD), denoted by $S_i(f)_n^{ch}$, for each of the persistent channel conductance states n is nearly frequency-independent within experimental error limits (Fig. 2 *A*). This white noise level

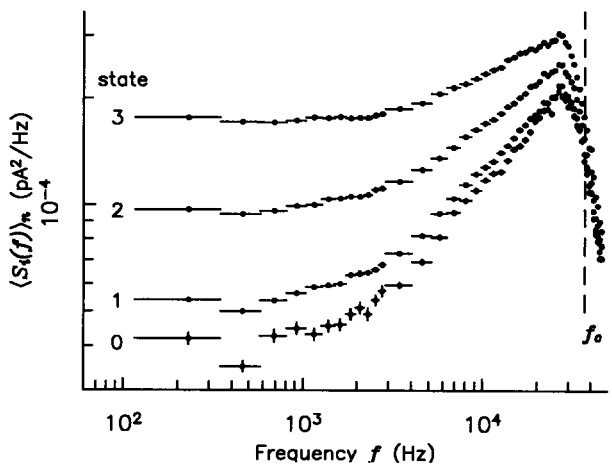

FIGURE 1 Mean current power spectra $\langle S_i(f)\rangle_n$ of various persistent channel conductance states. f_c is the 3-dB frequency of the anti-aliasing 4-pole Bessel filter (37 kHz). The NaCl concentration in the buffer solution was 1.0 M. Applied potential was +60 mV.

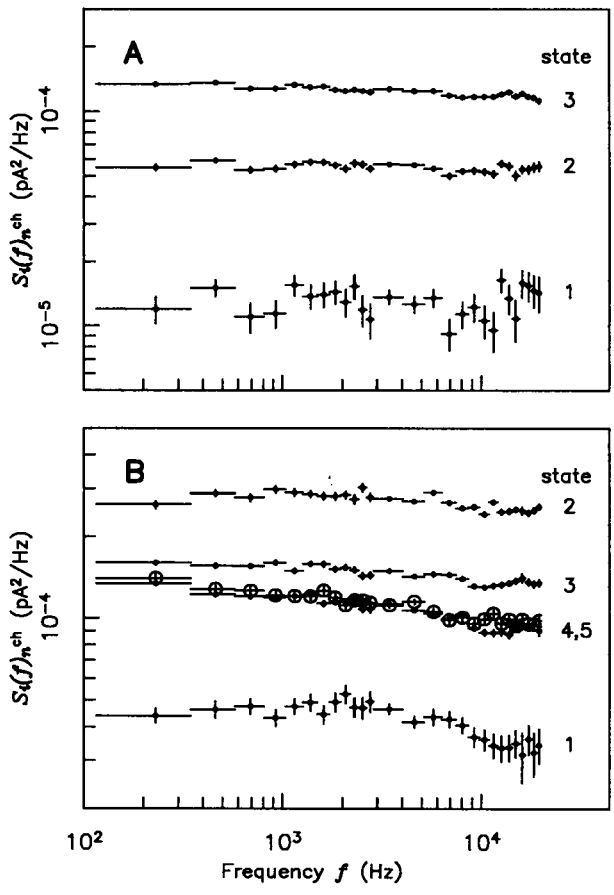

FIGURE 2 Channel current noise spectra $S_i(f)_n^{ch}$ of various conductance states with instrumental background noise spectrum $\langle S_i(f)\rangle_o$ removed. Buffer NaCl concentration was 1.0 M. (*A*) Spectra for persistent channel at 60 mV. (*B*) Spectra for nonpersistent channel at −68 mV. In *B*, the spectra for states 4 and 5 (*open circles*) are very close to each other.

increases for higher conductance states in persistent channels.

Nearly white current noise spectra are also found for nonpersistent channels (Fig. 2 *B*). The dependence of the noise level on the conductance state n in nonpersistent channels does not follow a simple trend. At the applied voltage used for Fig. 2 *B*, conductance states 2 and 3 have higher noise levels than states 4 and 5. The decrease of noise level from state 2 to state 4 agrees with results obtained by Bezrukov and Vodyanoy (1991) using black lipid membrane. (State 2 in our description corresponds to level 1 in Bezrukov and Vodyanoy's paper.)

Because the noise spectra for both persistent and nonpersistent channels are nearly white in the 100 Hz to 20 kHz range, we can represent the level of the channel current noise in that frequency range effectively by a characteristic PSD value $[S_i]_n^{ch}$ obtained by averaging $S_i(f)_n^{ch}$ over the frequencies between 100 Hz and 20 kHz.

The channel current PSD $[S_i]_n^{ch}$ increases monotonically with the channel current level i_n^{ch} for all conductance states in persistent channels under all applied potentials (Fig. 3 *A*). For nonpersistent channels, $[S_i]_n^{ch}$ only increases with the channel current level for higher conductance states (Fig. 3 *B*). $[S_i]_n^{ch}$ for conductance states 2 and 3 are exceptionally high for their current levels. Depending on the applied potential, state 3 $[S_i]_n^{ch}$ may be larger (Fig. 2 *B*) or smaller (Fig. 3 *B*) than state 4 $[S_i]_n^{ch}$. In general, in higher conductance states, $[S_i]_n^{ch}$ of a persistent channel is much greater than $[S_i]_n^{ch}$ of a nonpersistent channel in the corresponding state under similar experimental conditions.

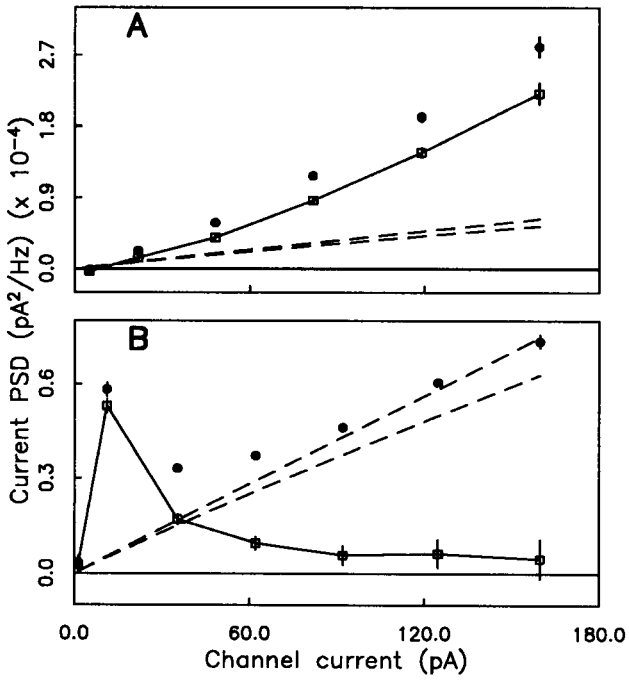

FIGURE 3 Graphs of current PSD versus channel current for (*A*) a persistent channel and (*B*) a nonpersistent channel. Filled circles are total channel current PSD $[S_i]_n^{ch}$. The dashed lines indicate the range of the calculated current PSD due to Johnson and shot noises $[S_i]_n^{J\&s}$. Open boxes connected by solid line are the difference between the two. Applied potential was +44 mV for *A*; +37 mV for *B*. Buffer NaCl concentration was 1.0 M.

EVALUATION OF BACKGROUND NOISE SOURCES

There are several possible contributions to the measured channel current noise:

a. Noise arising from short unresolved current pulses produced by the channel undergoing brief $n \rightarrow (n \pm 1) \rightarrow n$ transitions (Colquhoun and Sigworth, 1983);
b. Johnson-Nyquist noise (Nyquist, 1928) due to thermal agitation of charge carriers in the spreading resistance around the channel (Holm, 1967; Symthe, 1967);
c. Shot noise due to discrete, thermally activated movement of individual ions across the channel (Laüger, 1975; DeFelice, 1981a);
d. Fluctuations in the local conductivity of the electrolyte inside the channel and in the surrounding region due to stochastic ion concentration fluctuation via random ion diffusion (van Vliet and Fassett, 1965; Voss and Clarke, 1976; Bezrukov and Vodyanoy, 1991);
e. Fluctuations in the shape and size of the channel pore due to thermal excitation of both the arrangement of alamethicin molecules in the channel aggregate and the conformation of individual alamethicin molecules (Stevens, 1972; Sigworth, 1985; Laüger, 1985).

Both d and e cause fluctuations in the conductance of the channel. To extract the current fluctuations due to thermal molecular motions from the measured channel current noise, the background noise sources a to d must be individually evaluated and excluded.

Noise due to unresolved conductance state transition events

When an observed alamethicin channel undergoes pairs of conductance state transitions $n \rightarrow (n \pm 1) \rightarrow n$ in rapid succession so that the channel returns to the initial state, pulses are generated in the channel current record. Because of the limited response time of our data acquisition and analysis system, very brief current pulses generated by such conductance state transition events are indistinguishable from regular current fluctuations that occur while the channel is staying continuously in the same state (Colquhoun and Sigworth, 1983). Part of the noise in the channel current is due to these undetected events (Sigworth et al., 1987). To estimate the contribution of these events to the total measured channel current noise, we characterize the kinetics of the conductance state transition process within our observable time scale by constructing the dwell-time distribution histograms of the channel (Sigworth and Sine, 1987). Assuming that the kinetics of the state transition process in the

time scale just below the time resolution of the equipment is not radically different from that observed, it is possible to estimate the contribution of undetected state transitions to the total channel current noise. The following evaluation will show that this contribution is negligible in our experiments.

Fig. 4 *A* shows the dwell-time distribution histogram of "up pulses" with transition sequence 1→2→1 for a typical persistent channel and is representative for "up pulses" of all persistent channel conductance states. Because our experimental conditions were specially chosen to reduce the frequency of conductance state transitions (Boheim, 1974; Gordon and Haydon, 1976; Boheim and Kolb, 1978) so that more samples of current noise spectra could be collected, the total number of state transitions observed in any one experimental record was not very large. The probability density function (Sigworth and Sine, 1987) $f_n^{\uparrow}(\tau)$ consists of two distinct exponential components (Opsahl, 1993) whose time constants are well separated and much shorter than the total length T of the current record. Even though the kinetic parameters obtained directly from the dwell-time distribution have small errors due to missed events (Colquhoun and Hawkes, 1983; Magleby and Weiss, 1990), the accuracy of those parameters without any further correction is sufficient for our estimating purpose.

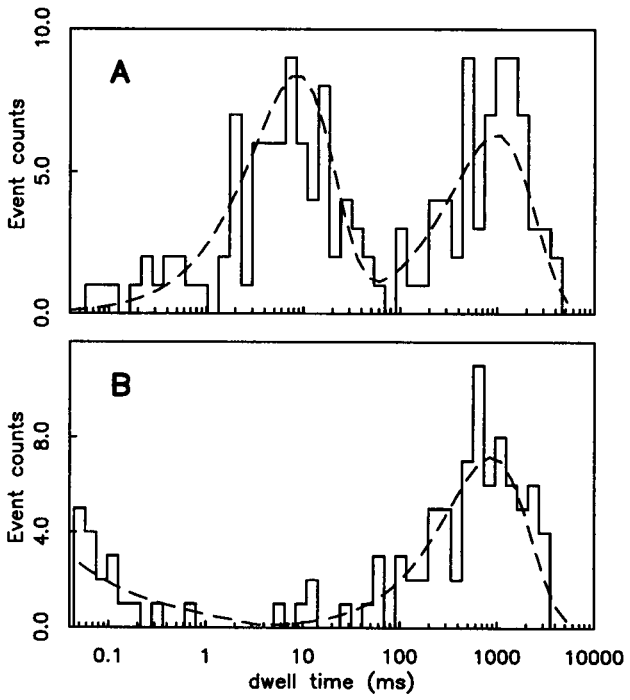

FIGURE 4 Dwell-time distribution histograms for a typical persistent channel in conductance state 2 under applied potential of 34 mV and buffer NaCl concentration of 1.0 M. (*A*) Histogram for events with transition sequence 1 → 2 → 1. The dashed curve is the theoretical probability density function $f_n^{\uparrow}(\tau)$ with two exponential components fitted by maximizing the logarithm of the likelihood (Sigworth and Sine, 1987) using the simplex algorithm (Caceci and Cacheris, 1984; Press, et al., 1987b). Total number of events counted = 150 in 200 s. (*B*) Histogram for events with transition sequence 3 → 2 → 3. The dashed curve is the theoretical probability density function $f_n^{\downarrow}(\tau)$ described by Eq. 2. The dwell-time distribution for events shorter than 1 ms is nonexponential. Total number of events counted = 99 in 200 s.

Assuming that the kinetics of the state transition process characterized does not change drastically at shorter time scales, the total number $[N_n^{\uparrow}]_{tot}$ of "up pulses" of any duration can be determined in terms of the number $[N_n^{\uparrow}]_{obs}$ of "up pulses" detected in the current record. $[N_n^{\uparrow}]_{obs}/[N_n^{\uparrow}]_{tot} \approx \int_{\epsilon}^{T} f_n^{\uparrow}(\tau)\,d\tau$, where ϵ is the minimum pulse duration detected by the data analysis process. Using our data analysis software to analyze simulated current records with artificially generated pulses of various durations, ϵ was found to be about 0.04 ms. If $P_{(n-1)}$ is the relative occupation probability of state $(n-1)$, the channel is in state $(n-1)$ for a total time of $TP_{(n-1)}$. Within that time, the rate $\nu_{(n-1)}^{\uparrow}(\tau)$ of occurrence of "up pulses" of duration τ is

$$\nu_{(n-1)}^{\uparrow}(\tau) = \frac{[N_n^{\uparrow}]_{tot}}{TP_{(n-1)}} f_n^{\uparrow}(\tau)\,\delta\tau,$$

assuming that the channel is stationary.

An "up pulse" with $(n-1) \rightarrow n \rightarrow (n-1)$ transitions produces a current pulse of amplitude $[i_n^{ch} - i_{(n-1)}^{ch}]$ and contributes to the current noise of state $(n-1)$. Representing the current pulse as a square pulse of the same duration and amplitude, the total contribution of undetected "up pulses" to the current noise spectrum is

$$S_i(f)_{(n-1)}^{\uparrow} = \frac{2[N_n^{\uparrow}]_{tot}}{TP_{(n-1)}} \int_0^{\epsilon} f_n^{\uparrow}(\tau)[i_n^{ch} - i_{(n-1)}^{ch}]^2 \frac{\sin^2(\pi f\tau)}{(\pi f)^2}\,d\tau \quad (1)$$

This contribution was estimated to be about 5 to 7 orders of magnitude smaller than the values of $S_i(f)_n^{ch}$ measured, even when the worst-case parameters were used.

The dwell-time distribution of the "down pulses" is very different from that of the "up pulses." The probability density function is (Opsahl, 1993)

$$f_n^{\downarrow}(\tau) = \frac{a_n}{\tau_n}\exp\left(\frac{-\tau}{\tau_n}\right) + k_n\tau^{-3/2}, \quad (2)$$

within the observable time scale (Fig. 4 *B*). The two components in $f_n^{\downarrow}(\tau)$ are well apart and $\tau_n \gg \epsilon$ for all conductance states n. It has been shown in our analysis of "up pulses" that the exponential component does not contribute significantly to the current noise. Therefore, we concentrate on the pulses in the nonexponential part of $f_n^{\downarrow}(\tau)$ with durations $<0.01\tau_n$. The $\tau^{-3/2}$ relation cannot be true for arbitrarily small values of τ. Because the contribution of short pulses to the current noise is directly proportional to the square of their durations, extremely short pulses have little significance to our noise analysis. Therefore, with no available information on the behavior of $f_n^{\downarrow}(\tau)$ at $\tau < \epsilon$, we can adopt a convenient form of $f_n^{\downarrow}(\tau)$ for very short pulses without affecting the outcome of our evaluation:

$$f_n^{\downarrow}(\tau) \approx \begin{cases} 0 & \tau < \zeta \\ \zeta^{1/2}\tau^{-3/2}/2 & \zeta \le \tau < 0.01\tau_n \end{cases}.$$

This implies that no "down pulse" has a duration shorter than ζ. A reasonable value for ζ is ~0.1 μs, the time taken for an alamethicin molecule to diffuse a distance of 6.5 Å (the molecular radius from Schwarz and Savko, 1982) away from the channel-forming aggregate so that a change of conductance state can occur. If $[N_n^{\downarrow}]_{obs}$ is the number of detected events with $\tau < 0.01\tau_n$, then the total number $[N_n^{\downarrow}]_{tot}$ of "down pulses" due to the nonexponential component of $f_n^{\downarrow}(\tau)$ is given by $[N_n^{\downarrow}]_{tot} \approx (\epsilon/\zeta)^{1/2}[N_n^{\downarrow}]_{obs}$. The contribution of undetected "down pulses" with $(n + 1) \rightarrow n \rightarrow (n + 1)$ transitions to the current noise of state $(n + 1)$ can be estimated with an equation similar to Eq. 1. Even with worst-case parameters, this was 3 to 5 orders of magnitude smaller than the current noise measured.

Similar kinetics for state transition was found for nonpersistent channels with probability density functions similar to those of persistent channels (data not shown). This indicates that the mechanisms for conductance state transitions in persistent and nonpersistent channels are probably similar and supports the "reversed-molecule" model described in our preceding paper (Mak and Webb, 1995), in which both persistent and nonpersistent channels undergo conductance state transition by having a single alamethicin molecule join or leave the channel aggregate. The current noise due to undetected state transition events in nonpersistent channels has a magnitude similar to that in persistent channels.

With the estimated current noise caused by undetected state transition events for both persistent and nonpersistent channels several orders of magnitude smaller than the measured channel current noise $[S_i]_n^{ch}$, we can reasonably conclude that the undetected brief pulses (up or down) are not a significant source of current noise in alamethicin channels.

Intrinsic Johnson and shot noises

To evaluate the shot noise in an alamethicin channel, we use the theory proposed by Laüger (1975). The transport of ions across the alamethicin channel was considered as independent, thermally activated, bidirectional movement of ions across the channel, like the movement of electrons across a saturated thermionic diode. Using the equations for the forward and reversed ion transport in (Laüger, 1975), the channel current can be expressed as

$$i_n^{ch} = e_o A_n \bar{\rho} \frac{kT}{h}\left[2\sinh\left(\frac{v}{2}\right)\right]\left[\exp\left(\frac{-E_n^+}{kT}\right) + \exp\left(\frac{-E_n^-}{kT}\right)\right],$$

where k is Boltzmann's constant, T the temperature of the system, h Planck's constant, A_n a proportionality constant, and $\bar{\rho}$ the ion concentration on both sides of the bilayer. E_n^+ and E_n^- are energy barriers encountered by cations and anions in the channel, respectively, and v is the reduced potential energy $= e_o V_{ch}/kT$, where V_{ch} is the potential drop across the channel. V_{ch} is smaller than the applied potential V_{ap} because of the spreading resistance of the buffer around the channel (Holm, 1967). The spreading resistance R_n^{sp} is given by

$$i_n^{ch} R_n^{sp} = V_{ap} - V_{ch} = (1 - c_n)V_{ap},$$

where $c_n < 1$ and is different in various conductance states, depending on the channel pore size (Mak and Webb, 1995).

Assuming that the rates of forward and reverse transport of cations and anions across the channel are independent and applying Campbell's theorem (DeFelice, 1981b), the current thermal shot noise spectral density $[S_i]_n^s$ for conductance state n is

$$[S_i]_n^s = 2e_o^2 A_n \bar{\rho} \frac{kT}{h}\left[2\cosh\left(\frac{v}{2}\right)\right]\left[\exp\left(\frac{-E_n^+}{kT}\right) + \exp\left(\frac{-E_n^-}{kT}\right)\right]$$
$$= 2e_o i_n^{ch} \coth(v/2). \quad (3)$$

For $1 \ll v$, $\coth(v/2) \rightarrow 1$, Eq. 3 becomes Schottky's formula (Schottky, 1918): $[S_i]_n^s = 2e_o i_n^{ch}$. At the low applied potential limit $v \rightarrow 0$, $\coth(v/2) \rightarrow 2/v$, Eq. 3 then gives the familiar formula for Johnson current noise (Nyquist, 1928): $[S_i]_n^s = 4kT\, i_n^{ch}/V_{ch} = 4kT/R_n^{ch}$, where R_n^{ch} is the resistance of the channel itself.

Besides noise in the channel resistance, the noise in the spreading resistance R_n^{sp} around the channel must also be taken into consideration. The spreading resistance is assumed to be ohmic, so the noise in it is simple Johnson noise. Because the channel resistance R_n^{ch} is in series with the spreading resistance R_n^{sp}, fluctuation in potential across the channel due to the shot noise $[S_v]_n^s$ and fluctuation in the potential across the spreading resistance due to Johnson noise $[S_v]_n^J$ are independent.

$$[S_v]_n^s = [S_i]_n^s \left(\frac{\partial V_{ch}}{\partial i_n^{ch}}\right)^2 = \left(\frac{8k^2T^2}{e_o i_n^{ch}}\right)\tanh\left(\frac{v}{2}\right),$$

and

$$[S_v]_n^J = 4kT(R_n^{sp}) = 4kT[(1 - c_n)V_{ch}/(c_n i_n^{ch})].$$

The Johnson and shot noise in the channel current $[S_i]_n^{J\&s}$ is

$$[S_i]_n^{J\&s} = ([S_v]_n^J + [S_v]_n^s)\left(\frac{\partial i_n^{ch}}{\partial V_{ch}}\right)^2 c_n^2$$
$$= e_o c_n i_n^{ch}[(1 - c_n)v\coth^2(v/2) + 2c_n\coth(v/2)]. \quad (4)$$

The first term is due to Johnson noise in the spreading resistance and the second term is due to shot noise in the channel. This noise is white (frequency independent) inasmuch as both Johnson and shot noises are white. The values of the current noise PSD due to Johnson and shot noises $[S_i]_n^{J\&s}$ calculated with Eq. 4 were plotted in Fig. 3. The error ranges of $[S_i]_n^{J\&s}$ indicated in Fig. 3 come mainly from the uncertainty in evaluating c_n (Mak and Webb, 1995) from experimental data (Taylor and de Levie, 1991).

According to our model, the shot noise and the Johnson noise in the channel with the energy barrier are one and the same, given by $[S_i]_n^s$ in Eq. 3. Other models that regard the channel as a simple resistance give independent shot noise

and Johnson noise in the channel resistance. Then the total Johnson and shot noise in the current will be overestimated, so $[S_i]_n^{J\&s}$ is greater than the measured channel noise $[S_i]_n^{ch}$ for the higher conductance states in nonpersistent channels.

As the contribution from missed channel transition events was shown to be insignificant, the difference $[\Delta S_i]_n$ between the measured channel current noise PSD $[S_i]_n^{ch}$ and the calculated Johnson and shot noises $[S_i]_n^{J\&s}$ is caused by channel conductance fluctuations. This difference is also plotted in Fig. 3. In persistent channels, this difference increases monotonically from lower to higher conductance states. In nonpersistent channels, the difference is mainly found in the lower conductance states, whereas the Johnson and shot noises are the major contributions to the total channel current noise in higher conductance states.

Ion concentration fluctuation noise

Part of the measured current noise above the Johnson and shot noises is due to electrolyte concentration fluctuation. Spontaneous, random diffusion of ions in the vicinity of the channel can produce fluctuations in the local electrolyte concentration. Assuming that the conductivity of the buffer solution is directly proportional to its ion concentration, the ion concentration fluctuations cause fluctuations in the local conductivity around the channel where high current flux flows through. This results in fluctuations in the conductance Λ_n of the channel system. At the same time, Λ_n also fluctuates because of fluctuations in the shape and size of the channel pore caused by intermolecular thermal motions of the alamethicin molecules in the channel aggregate and intramolecular thermal motions inside each alamethicin molecule. Because both persistent and nonpersistent channels are ohmic within our experimental range of applied voltage (Mak and Webb, 1995), the PSD $[S_\Lambda]_n$ of the fluctuations in the channel conductance Λ_n can be expressed as

$$\frac{[S_i]_n^{ch} - [S_i]_n^{J\&s}}{(i_n^{ch})^2} = \frac{[\Delta S_i]_n}{(i_n^{ch})^2} = \frac{[S_\Lambda]_n}{(\Lambda_n)^2} = S_n^{ion} + S_n^{mol},$$

where S_n^{ion} and S_n^{mol} are the dimension-free normalized PSD due to ion concentration fluctuation and thermal molecular motion, respectively. $[\Delta S_i]_n/(i_n^{ch})^2$ was found to be voltage and current independent because $[S_\Lambda]_n/(\Lambda_n)^2$ has no direct voltage or current dependence.

In an upcoming paper (in preparation), we show from theoretical derivation from first principles that the normalized noise PSD caused by ion concentration fluctuation $S_n^{ion} = G_n/(D\bar{\rho})$, where D is the diffusion coefficient of the ion inside the channel, $\bar{\rho}$ is the mean buffer electrolyte concentration, and G_n is a geometric factor controlled by the shape and size of the channel.

Fig. 5 shows the graphs of the normalized excess noise PSD $[\Delta S_i]_n/(i_n^{ch})^2$ versus the inversed buffer ion concentration $1/\bar{\rho}$ for various conductance states of nonpersistent channels. Within experimental error limits, the linear relation holds between $\bar{\rho} = 0.33$ and 2.0 M. The slopes α_n of

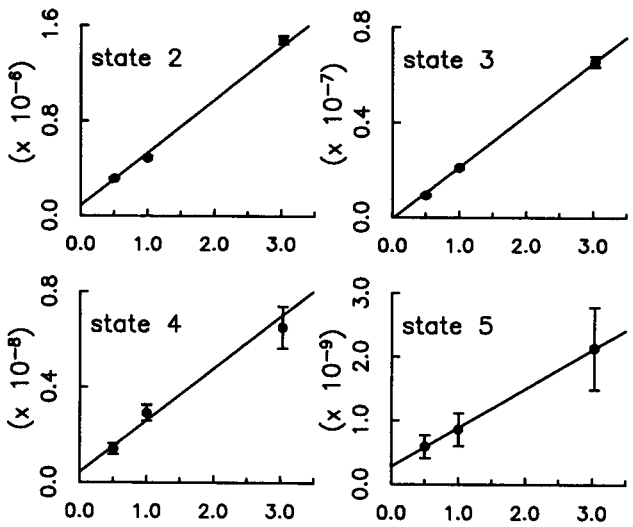

FIGURE 5 Graphs of the normalized excess noise PSD $[\Delta S_i]_n/(i_n^{ch})^2$ (Hz^{-1}) versus the inversed buffer ion concentration $1/\bar{\rho}$ (M^{-1}) for various nonpersistent channel conductance states.

those graphs vary over nearly four orders of magnitude. The slopes α_n for persistent channels were found with similar procedures. Fig. 6 shows the slopes α_n for various conductance states plotted against the channel conductance values Λ_n in 1.0 M NaCl buffer solution. The slopes α_n for fewer persistent channel conductance states found as persistent channels were rare and occurred in less than 5% of our experiments (Mak and Webb, 1995).

In the lowest two nonpersistent channel conductance states, the measured values of α_n were nearly an order of magnitude higher than those for persistent channels of comparable conductance value. This probably reflects the difference between the geometries of the nonpersistent and persistent channels. According to the "reversed-molecule"

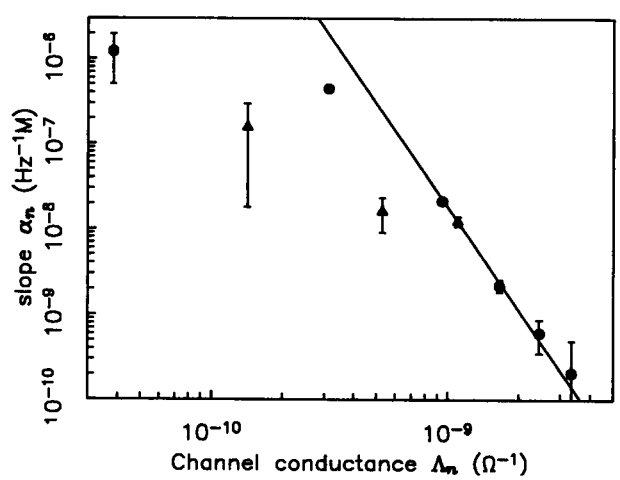

FIGURE 6 Graph of the slope α_n for various conductance states versus the channel conductance Λ_n in 1.0 M NaCl buffer solution at 7°C. Circles are data from nonpersistent channels (states 1–7). Triangles are data from persistent channels (states 1–3). The solid line represents the empirical relation $\alpha_n = \gamma(\Lambda_n)^{-4}$ for higher conductance states ($n > 2$).

model proposed in our preceding paper (Mak and Webb, 1995), nonpersistent channels differ from persistent ones by containing a reversed molecule aligned antiparallel to other alamethicin monomers forming the channel. This can distort the arrangement of alamethicin molecules from the highly symmetric persistent channel configuration described by the "barrel-stave" model (Baumann and Mueller, 1974). The distortion may create regions in the channel pore in which the movement of the ions is very restricted and reduce the effective diffusion coefficient D of the ions inside the channel (Levitt, 1974; Levitt and Subramanian, 1974), thus increasing the value for α_n. However, this effect cannot be quantified because of the lack of structural information about the nonpersistent channels.

As the number of alamethicin molecules present in the channel aggregate increases in higher conductance states according to the barrel-stave model (Baumann and Mueller, 1974; Boheim, 1974), the influence of the reversed molecule on the channel geometry evidently becomes less significant so that by state 3, α_3 for persistent and nonpersistent channels are not very different.

In higher conductance states ($n > 2$), α_n for both persistent and nonpersistent channels appear to vary with the channel conductance as

$$\alpha_n = \gamma(\Lambda_n)^{-4}. \quad (5)$$

This is a purely empirical relation that reflects the decrease in G_n due to both the direct effect of the increase in channel pore size and a change in the relative significance of the spreading resistance and channel resistance as the channel pore size changes.

THERMAL MOLECULAR MOTIONS IN ALAMETHICIN CHANNELS

Channel current noise due to spontaneous thermal molecular motions

To remove the contribution to the normalized excess channel noise PSD $[\Delta S_i]_n/(i_n^{ch})^2$) by ion concentration fluctuation (S_n^{ion}), the $[\Delta S_i]_n/(i_n^{ch})^2$ versus $1/\bar{\rho}$ graphs for various conductance states in Fig. 5 were extrapolated to obtain the y-intercepts. This is the normalized excess channel noise PSD remaining at infinite buffer ion concentration, where there can be no more concentration fluctuation. For those high conductance states with insufficient data points to give accurate y-intercept values directly, the y-intercepts were estimated by using α_n derived from the empirical relation Eq. 5. With all other possible contributions to channel noise thus methodically removed, the channel noise left is assumed to be due to fluctuation in the channel conductance caused by thermal molecular motion in the channel aggregate (S_n^{mol}). Figs. 7 and 8 show, for nonpersistent and persistent channels respectively, the graphs of S_n^{mol} versus a measure of the effective channel radius defined in terms of the maximum permeable ion radii r_n^{max}, the radii of the largest ion that can pass through the channel in state n as

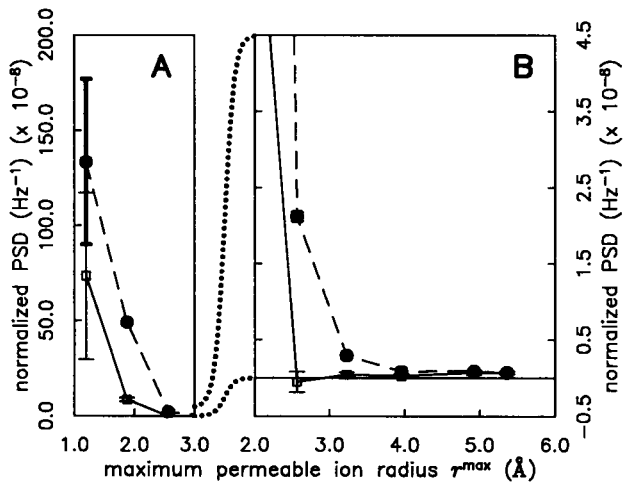

FIGURE 7 Graph of normalized PSD $[\Delta S_i]n/(i_n^{ch})^2$ and S_n^{mol} versus maximum permeable ion radii r_n^{max} for nonpersistent channel conductance states 1 to 7. Filled circles connected by dashed line are $[\Delta S_i]_n/(i_n^{ch})^2$, at buffer NaCl concentration of 1.0 M. Open boxes connected by solid line are S_n^{mol}.

calculated from the molecular models for the alamethicin channels proposed in our preceding paper (Mak and Webb, 1995). The values of the normalized excess current PSD $[\Delta S_i]_n/(i_n^{ch})^2$ in buffer with 1.0 M NaCl are also plotted for comparison. The difference between the two values indicates the magnitude of S_n^{ion} and α_n as $1/\bar{\rho}$ is simply 1.0 M^{-1}.

In Fig. 7, a different scale is used for states 1 and 2 because S_n^{mol} and S_n^{ion} are very large compared with values for higher nonpersistent states. Beyond state 2, both S_n^{mol} and S_n^{ion} drop precipitously, resulting in nonpersistent channel current being much quieter than persistent channel current in higher conductance states (Fig. 3 *B*).

In persistent channels, the values of S_n^{mol} settle to a stable and definitely nonzero value in higher conductance states

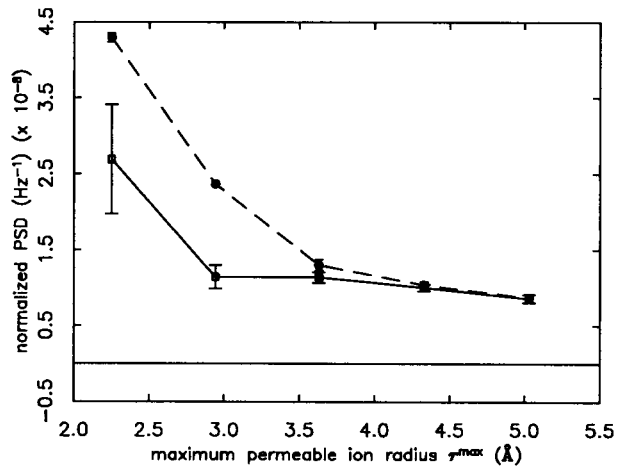

FIGURE 8 Graph of normalized PSD $[\Delta S_i]_n/(i_n^{ch})^2$ and S_n^{mol} versus maximum permeable ion radii r_n^{max} for persistent channel conductance states 2 to 6. Same convention for symbols as Fig. 7. Scale for y-axis is the same as for Fig. 7 *B*.

(Fig. 8). With the drop in S_n^{ion} in higher conductance states, S_n^{mol} becomes the major contribution to the conductance fluctuation noise. The large channel current i_n^{ch} in the higher conductance states amplifies the effect of these molecular fluctuations on the total channel current noise, resulting in the increasing channel current noise in higher states in Fig. 3 *A*.

Analysis of molecular fluctuations in the channel

Despite its relatively simple structure, there are many possible molecular thermal motions in an alamethicin channel aggregate that can affect its shape and therefore its conductance, including:

i. translational motion of the alamethicin monomers in a radial direction outward from the channel pore;
ii. translational or rotational vibration of the amino acid side chains, particularly Gln^7, that protrude from the main alamethicin helices into the channel pore to form the constriction in the channel pore (Sansom, 1993);
iii. bending deformation of the alamethicin helix at the flexible "hinge" formed by Pro^{14} that disrupts the rigid alamethicin helix structure (Fraternali, 1990; Vogel et al., 1993);
iv. "twisting" motion of the alamethicin helices similar to the kind that is responsible for gating of gap junctions according to Unwin and Zampighi (1980).

These various possible molecular oscillations are coupled directly and indirectly by intermolecular and intramolecular interactions. Thus, there are many different normal modes of oscillation (Landau and Lifshitz, 1976). To simplify the picture, we observe that in the molecular models proposed in our preceding paper (Mak and Webb, 1995), the channel conductance is mainly controlled by the size of the channel pore at the pore constriction, where side chains from Gln^7 protrude from the main alamethicin helices into the aqueous channel pore. The size of that pore constriction is in turn determined mostly by x_j, the distance from the axis of the channel to the protruding Gln^7 side chain of the jth alamethicin monomer in the channel aggregate. The pore size and therefore the channel conductance fluctuate most when all the Gln^7 side chains are oscillating in concert, so that $x_j = x$ for all j all of the time. We assume, for simplicity, that in some normal modes of molecular oscillation, the side chains do oscillate in concert so that x ($= x_j$ for all j) is a normal coordinate. Considering the large number of degrees of freedom for oscillations, there is probably more that one such "concerted" normal mode. For a "concerted" normal mode, we can write a representative Langevin equation of motion (Langevin, 1908; Chandrasekhar, 1943; Adelman, 1980): $m\ddot{x} + \beta_x x + \kappa_x x = F_x(t)$, where $F_x(t)$ is the random thermal perturbation. This approach is similar to the one used by Laüger (1985) in considering protein domain oscillation. It should be noted that in the equation, κ_x is the force constant, β_x is the damping constant, and m is an effective mass for a specific normal mode of oscillation. The value of κ_x depends on the many interactions inside the complex channel environment and changes from one normal mode to another. We limit our consideration to the normal mode with the minimum κ_x and therefore the maximum oscillation amplitude in x, assuming that fluctuation in channel conductance caused by this mode of oscillation overwhelms the other modes. Using the Fourier transform of the Langevin equation, the PSD of the oscillation is

$$S_x(\omega) = \frac{2|\mathcal{F}_x|^2}{[\kappa_x - m_x\omega^2]^2 + [\beta_x\omega]^2},$$

where $\mathcal{F}_x$, the Fourier transform of $F_x(t)$, is frequency independent, as the thermal perturbation is random and uncorrelated. By Parseval's theorem and the equipartition of energy,

$$\kappa_x\langle x^2\rangle = \kappa_x \int_0^\infty S_x(\omega)\, d\omega = kT \tag{6}$$

where $\langle x^2\rangle$ is the mean square oscillation amplitude about the equilibrium distance of the protruding Gln^7 side chains from the channel pore axis. For molecular motions that we are considering, $(\beta_x)^2$ is usually $\gg 2m_x\kappa_x$ (Laüger, 1985), so the roll-off frequency of the molecular oscillation $f_o \approx \kappa_x/2\pi\beta_x$ and $|\mathcal{F}_x|^2 = 2kT\,\beta_x$ (Eq. 6). Because the current noise PSD found for alamethicin channels is nearly white in the observed frequency range, $f_o \gg 20$ kHz and $S_x(\omega) \approx (4kT\,\beta_x)/(\kappa_x)^2$ for all frequencies in our observed range.

The molecular motion PSD $[S_x]_n$ for channel state n is related to the normalized noise PSD S_n^{mol} by

$$S_n^{mol} = \frac{[S_x]_n}{(\Lambda_n)^2}\left(\frac{\partial\Lambda_n}{\partial x}\right)^2. \tag{7}$$

The factor $\partial\Lambda_n/\partial x$ expresses the dependence of the channel conductance Λ_n on the positions of the protruding side chains. From our preceding paper (Mak and Webb, 1995), the equivalent channel pore radius r_n^{eq} is defined as the radius of a circular pore with the same spreading resistance (Holm, 1967) as the channel. The conductance of the channel itself is empirically found to be directly proportional to $\pi(r_n^{eq})^2$. Therefore,

$$\frac{1}{\Lambda_n} = \frac{1}{K\pi(r_n^{eq})^2} + \frac{1}{2\bar{\sigma}r_n^{eq}},$$

where K is an experimentally derived proportionality constant and $\bar{\sigma}$ the mean conductivity of the buffer. The first term is the resistance of the channel itself and the second term the spreading resistance around the channel.

$$\frac{\partial\Lambda_n}{\partial x} = \frac{\Lambda_n}{r_n^{eq}}\left(1 + \frac{\Lambda_n}{K\pi(r_n^{eq})^2}\right)\left(\frac{\partial r_n^{eq}}{\partial x}\right). \tag{8}$$

Because the distance x of the protruding side chains from the channel axis changes the channel pore radius directly,

we could use an extreme simplification and assume that $(\partial r_n^{eq}/\partial x) = 1$. A more sophisticated but model-dependent approach used here assumes the molecular models of the alamethicin channel developed in our preceding paper (Mak and Webb, 1995). The channel conducting pore area can be calculated using the models in terms of x. If the equivalent area of the channel $\pi(r_n^{eq})^2$ is assumed to be the same as the model conducting area, then $(\partial r_n^{eq}/\partial x)$ can be derived. As the symmetry of the channel increases with the number of alamethicin monomers in the channel, $(\partial r_n^{eq}/\partial x)$ approaches 1 in higher conductance states. It deviates from 1 in lower states, but only significantly (>30%) in states 1 and 2 for nonpersistent channels (= 1.8 and 1.4 for n = 1 and 2, respectively).

Using Eq. 8 and Eq. 7,

$$\kappa_n \sqrt{\beta_n} = \left(\frac{4kT}{S_n^{mol}}\right)^{1/2} \left[\frac{1}{r_n^{eq}}\left(1 + \frac{\Lambda_n}{K\pi(r_n^{eq})^2}\right)\right]\left(\frac{\partial r_n^{eq}}{\partial x}\right), \quad (9)$$

where κ_n and β_n are the molecular motion parameters for conductance state n. The time resolution of the equipment and more importantly the rise in instrumental background noise at high frequencies (Fig. 1) limit the frequency range observable in our experiments. The roll-off frequency of the relevant "concerted" normal mode of oscillation must lie above our observed frequency range because the current noise PSD for alamethicin channels we found is frequency independent. The magnitude of S_n^{mol} alone is insufficient to determine κ_n and β_n simultaneously. However, if we assume that the frictional coefficient does not change greatly in different conductance states $\beta_n \approx \beta$, we can find κ_n in terms of β and examine the relative magnitude of the force constants for various persistent and nonpersistent channel conductance states. Fig. 9 shows the graph of $(\kappa_n/\sqrt{\beta})$ (L.H.S. of Eq. 9) versus the maximum permeable ion radius r_n^{max} for persistent and nonpersistent channels. The data point for persistent channel state 1 was not plotted because its low occupation probability leads to large uncertainty in the value of S_1^{mol}.

From Fig. 9 it can be seen that the force constants κ_n for persistent channel states gradually decrease with no abrupt change as the channel size increases. We conclude that the interactions controlling the oscillation in the persistent channels are probably similar in nature throughout the various conductance states. The decrease in κ_n in higher conductance states means that larger channels are less stiff and can oscillate more, which is not unreasonable. κ_n reflects the resultant of many interactions (peptide-peptide, peptide-ion, peptide-water, peptide-lipid, and bilayer-water) inside the complex channel environment and is the force constant of a particular normal mode of oscillation, the exact nature of which we do not know. Thus, detailed quantitative interpretation of the trends of κ_n seen in Fig. 9 is not possible at this point.

In the two lowest nonpersistent channel states, κ_n is similar in magnitude to κ_n for persistent channels in similar states. This indicates that the nature of the interactions in

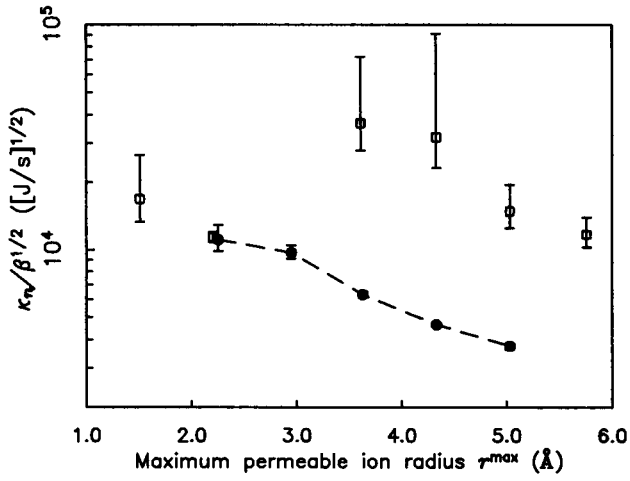

FIGURE 9 Graph of $\kappa_n(\beta)^{-1/2}$ versus maximum permeable ion radius r_n^{max} for various persistent and nonpersistent channel conductance states. Filled circles connected by dashed line are data from persistent channel states 2 to 6. Open boxes are data from nonpersistent channel states 1 to 7. Data point from nonpersistent channel state 3 is off scale.

nonpersistent channel states 1 and 2 is probably similar to that in persistent channels, although the large values of α_1 and α_2 evaluated from the ion concentration fluctuation analysis indicate that there is probably a large distortion of the nonpersistent channel geometry in these states. In higher nonpersistent conductance states, the picture is very different. S_n^{mol} are significantly smaller than those for corresponding persistent states. The value of S_3^{mol} is so low that κ_3 cannot be determined accurately. For states 4–7, κ_n is 4 to 7 times the value for persistent channels of similar size. This clearly indicates the onset of a new kind of interaction in the channel aggregate in higher nonpersistent channel states, making the channel more rigid. Although κ_n decreases as the nonpersistent channel goes from state 4 to 7, κ_n for higher nonpersistent states remains unmistakably and substantially higher than κ_n for persistent channels of similar size. This indicates that the new interaction in the nonpersistent channel aggregates remains as the channel increases in size, although according to our proposed "reversed-molecule" model (Mak and Webb, 1995), the effect of a reversed molecule in the channel aggregate on the channel structure should decrease as more molecules join the channel aggregate in higher conductance states. Better understanding of the channel structure, especially in nonpersistent channels, is needed for a satisfactory explanation of these observations.

If we assume that the molecular oscillations that generate the channel current noise involve translational movement of the alamethicin helices in the channel aggregate, then it is possible to make an order-of-magnitude estimate of the frictional coefficient β_x. The frictional coefficient β_T for the translational motion in a lipid bilayer of a cylindrical object spanning the bilayer (like the alamethicin molecule in the channel aggregate) was deduced from theoretical consideration (Saffman and Delbrück, 1975; Saffman, 1976). Using

a length of an alamethicin molecule of ≈35 Å, radius of the alamethicin helix of ≈6.5 Å (Schwarz and Savko, 1982), viscosity of lipid bilayer of ≈1 Poise (Quinn, 1981), and viscosity of water of 0.01 Poise, β_T for translational motion of alamethicin in lipid bilayer $\approx 7 \times 10^{-9}$ Nsm^{-1}. Assuming $\beta_x \sim \beta_T$ gives an estimate for the force constant κ_x of about 0.6 Nm^{-1}. This is a lower limit for force constants of molecular oscillations that affect the channel conductance. The corresponding roll-off frequency f_o is about 70 MHz. According to our modified barrel-stave model of alamethicin channels (Mak and Webb, 1995), diffusion of ions across the channel constriction of length ~2–5 Å takes $\sim 10^{-10}$ s $< (1/f_o)$. Thus, the flow of ions across the alamethicin channel can be used to probe the full frequency range of the thermal molecular oscillations theoretically.

Using Eq. 6, the translational oscillation amplitude can be estimated (Fig. 10). The estimated r.m.s. amplitude of the translational molecular oscillation $\sqrt{\langle x^2 \rangle}$ approximately equals the size of the channel pore represented by its maximum permeable ion radius, especially for the lower conductance states. With such a large oscillation amplitude, it is very likely that the polar interactions between the hydrophilic alamethicin side chains and the water and ions inside the aqueous channel pore and the apolar interactions between the hydrophobic alamethicin side chains and the lipid bilayer around the channel aggregate contribute significantly to the intermolecular interactions in the channel, in addition to the short-range Lennard-Jones interactions between adjacent alamethicin molecules. The alamethicin molecules in the channel wall are kept together despite the large amplitude of molecular oscillations to avoid exposing the polar buffer in the channel pore to the apolar lipid acyl chains or the hydrophobic alamethicin amino acid side chains. Molecular dynamics simulations (Fraternali, 1990) and energy minimization (Furois-Corbin and Pullman, 1988) done in a vacuum or uniform medium environment will be inadequate for molecules in the complex channel environment in which both polar (buffer solution) and apolar (lipid bilayer) media are in close proximity to the channel molecules. With the large amplitude of oscillation, the Gln^7 side chains of the alamethicin molecules protruding into the channel pore will approach one another very closely when the channel pore is contracting during the oscillation, especially in lower conductance states. Even though the side chains are not perfect hard bodies, oscillation of excessive amplitude would be prevented by strong, short-range Lenard-Jones repulsion, so the oscillations are probably not harmonic.

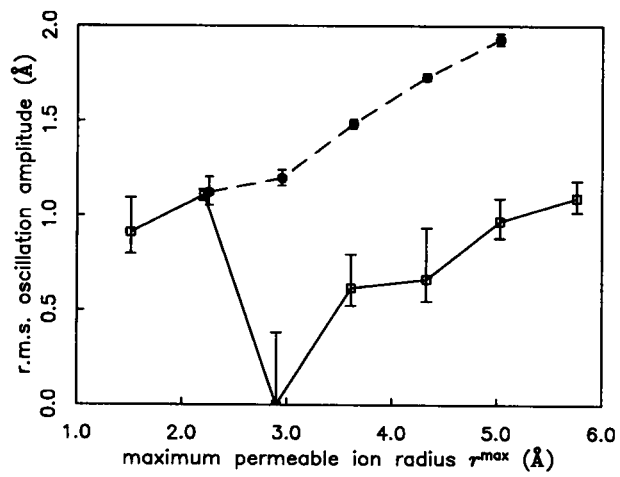

FIGURE 10 Graph of r.m.s. amplitude of translational molecular oscillations $\sqrt{\langle x^2 \rangle}$ versus maximum permeable ion radius r_n^{max} for persistent and nonpersistent channel conductance states. Filled circles connected by dashed line are from persistent channel states 2 to 6. Open boxes connected by solid line are from nonpersistent channel states 1 to 7.

On the other hand, we can assume that the oscillation of the protruding side chains is damped by peptide-peptide interaction, which may be significantly stronger than that due to lipid bilayer viscosity (Laüger, 1985). Assuming that the frictional coefficient β_x is of the same order of magnitude as that previously estimated for protein domain oscillations in acetylcholine receptors (Sigworth, 1985; Laüger, 1985), the damping would be 10^4 times larger with $\beta_x \sim 10^{-5}$ Nsm^{-1}. Then κ_x is found to be ~10 Nm^{-1} and $\sqrt{\langle x^2 \rangle}$ ~0.1 Å, which is significantly smaller than the channel pore dimension represented by r_n^{max}, so that the oscillation is probably harmonic. The roll-off frequency f_o in this case is ~100 kHz. Without further experimental information like the roll-off frequency or the actual amplitude of the alamethicin molecular oscillation, neither the model with strong frictional damping due to peptide-peptide interactions nor the one with weaker damping due to lipid bilayer viscosity can be discounted.

CONCLUSION

High-quality, low-instrumental-noise current records of single alamethicin channels in artificial lipid bilayers were obtained using patch-clamp technique under low temperature (7°C) that stabilizes the channel in one conductance state for extensive periods. After the background instrumental noise was removed, the current noise spectra found for all persistent and nonpersistent channel conductance states showed little frequency dependence within our observable frequency range of 100 Hz to 20 kHz.

To extract the channel current noise due to spontaneous thermal molecular motions in the alamethicin channel, contributions to the measured current noise due to other background noise sources must be removed. Current noise due to unresolved conductance state transitions was estimated using the observed channel dwell time distribution and found to be insignificant. Shot noise due to thermally activated, bidirectional ion transport across an energy barrier in the channel and Johnson noise in the spreading resistance around the channel were evaluated based on molecular models of the channel described in our preceding paper (Mak and Webb, 1995). Current noise due to buffer concentration fluctuation via random ion diffusion was isolated by its dependence on buffer ion concentration.

After removal of the background contributions, residual current noise, attributed to thermal molecular motions in the alamethicin channel causing fluctuation in the channel conductance, is observed in all persistent channel conductance states, and mainly in the lower conductance states of nonpersistent channels. Using our molecular models of the channel, the thermal molecular motions in the alamethicin channel are modeled by a Langevin translational oscillation of the channel-forming alamethicin molecules moving radially from the channel pore. Assuming that damping of this molecular oscillation is mainly due to lipid bilayer viscosity, we found that the amplitude of such molecular oscillation is substantial (~1–2 Å) and must be considered in molecular simulations of the channel.

We would like to thank T. Saido for pioneering work on alamethicin in artificial bilayers, L. R. Opsahl for useful discussions, S. Brundobler for developing data analysis software, and J. K. Foskett for help and support in the preparation of this manuscript.

This work was supported by a grant from the Office for Naval Research (N00014-89J-1656) and by facilities of the Developmental Resource for Biophysical Imaging and Optoelectronics provided by the National Institutes of Health (P41-RR04224) and the National Science Foundation (DIR 8800278).

REFERENCES

Adelman, S. A. 1980. Generalized Langevin equations and many body problems in chemical dynamics. *Adv. Chem. Phys.* 44:143–253.

Archer, S. J., J. F. Ellena, and D. S. Cafiso. 1991. Dynamics and aggregation of the peptide ion channel alamethicin. *Biophys. J.* 60:389–398.

Balasubramanian, T. M., N. C. E. Kendrick, M. Taylor, G. R. Marshall, J. E. Hall, I. Vodyanoy, and F. Reusser. 1981. Synthesis and characterization of the major component of alamethicin. *J. Am. Chem. Soc.* 103:6127–6132.

Baumann, G., and P. Mueller. 1974. A molecular model of membrane excitability. *J. Supramol. Struct.* 2:538–557.

Bezrukov, S. M., and I. Vodyanoy. 1991. Electrical noise of the open alamethicin channel. *In* Noise in Physical Systems and 1/*f* Fluctuations. T. Mushua, S. Sato, and M. Yamamoto, editors. Ohmsha, Ltd., Tokyo. 641–644.

Bezrukov, S. M., I. Vodyanoy, and V. A. Parsegian. 1994. Counting polymers moving through a single ion channel. *Nature.* 370:279–281.

Boheim, G. 1974. Statistical analysis of alamethicin channels in black lipid membranes. *J. Membr. Biol.* 19:277–303.

Boheim, G., and H.-A. Kolb. 1978. Analysis of the multi-pore system of alamethicin in a lipid membrane I. *J. Membr. Biol.* 38:99–150.

Caceci, M. S., and W. P. Cacheris. 1984. Fitting curves to data: the Simplex algorithm is the answer. *Byte.* May:340–348.

Cahalan, M., and E. Neher. 1992. Patch clamp techniques: an overview. *Methods Enzymol.* 207:3–14.

Chandrasekhar, S. 1943. Stochastic problems in physics and astronomy. *Rev. Mod. Phys.* 15:1–89.

Chou, K. C., and N. Y. Chen. 1977. The biological functions of low-frequency phonons. *Sci. Sin.* 20:447–457.

Chou, K. C., N. Y. Chen, and S. Forsén. 1981. The biological functions of low-frequency phonons. 2. Cooperative effects. *Chemica Scripta.* 18: 126–132.

Colquhoun, D., and A. G. Hawkes. 1983. The principles of the stochastic interpretation of ion-channel mechanisms. *In* Single-Channel Recording. E. Neher and B. Sakmann, editors. Plenum Press, New York and London. 135–176.

Colquhoun, D., and F. J. Sigworth. 1983. Fitting and statistical analysis of single-channel records. *In* Single-Channel Recording. E. Neher and B. Sakmann, editors. Plenum Press, New York and London. 191–263.

DeFelice, L. J. 1981a. Introduction to Membrane Noise. Plenum Press, New York and London. 329–330.

DeFelice L. J. 1981b. Introduction to Membrane Noise. Plenum Press, New York and London. 324–328.

Fraternali, F. 1990. Restrained and unrestrained molecular dynamics simulations in the NVT ensemble of alamethicin. *Biopolymers.* 30: 1083–1099.

Frauenfelder, H., and R. D. Young. 1986. Protein dynamics and ligand binding. *Comments Mol. Cell. Biophys.* 3:347–372.

Furois-Corbin, S., and A. Pullman. 1988. Conformation and pairing properties of the n-terminal fragments of trichorzianine and alamethicin: a theoretical study. *Biochim. Biophys. Acta.* 944:399–413.

Gordon, L. G. M., and D. A. Haydon. 1976. Kinetics and stability of alamethicin conducting channels in lipid bilayers. *Biochim. Biophys. Acta.* 436:541–556.

Gurd, R. N., and T. M. Rothgeb. 1979. Motions in proteins. *Adv. Protein Chem.* 33:73–165.

Hamill, O. P., A. Marty, E. Neher, B. Sakmann, and F. J. Sigworth. 1981. Improved patch-clamp techniques for high-resolution current recording from cells and cell-free membrane patches. *Pflüegers Arch. Eur. J. Physiol.* 391:85–100.

Hille, B. 1984. Ionic Channels of Excitable Membranes. Sinauer Associates, Sunderland, MA. 329–353.

Holm, R. 1967. Electric Contacts: Theory and Application. Springer-Verlag, Berlin and New York. 9–20.

Huber, R. 1979. Conformational flexibility and its functional significance in some protein molecules. *Trends Biochem. Sci.* 4:271–276.

Karplus, M. 1987. Molecular dynamics simulations of proteins. *Physics Today.* 40:68–72.

Karplus, M., and J. A. McCammon. 1983. Dynamics of proteins: elements and function. *Annu. Rev. Biochem.* 53:263–300.

Karplus, M., and G. A. Petsko. 1990. Molecular dynamics simulations in biology. *Nature.* 347:631–638.

Landau, L. D., and E. M. Lifshitz. 1976. Mechanics. Pergamon Press, Oxford. 65–70.

Langevin, P. 1908. Sur la théorie du movement Brownien. *C. R. Acad. Sci.* 146:530–534.

Latorre, R., and O. Alvarez. 1981. Voltage-dependent-channels in planar lipid bilayer membranes. *Physiol. Rev.* 61:77–150.

Laüger, P. 1975. Shot noise in ion channels. *Biochim. Biophys. Acta.* 413:1–10.

Laüger, P. 1985. Structural fluctuations and current noise of ionic channels. *Biophys. J.* 48:369–373.

Levitt, D. G. 1974. A new theory of transport for cell membrane pores. I. General theory and application to red cell. *Biochim. Biophys. Acta.* 373:115–131.

Levitt, D. G., and G. Subramanian. 1974. A new theory of transport for cell membrane pores. II. Exact results and computer simulation (molecular dynamics). *Biochim. Biophys. Acta.* 373:132–140.

Magleby, K. L., and D. S. Weiss. 1990. Estimating kinetic parameters for single channels with simulation. *Biophys. J.* 58:1411–1426.

Mak, D. D., and W. W. Webb. 1995. Two classes of transmembrane alamethicin channel: molecular models from single-channel properties. *Biophys. J.* In press.

Martin, D. R., and R. J. P. Williams. 1975. The nature and function of alamethicin. *Biochem. Soc. Trans.* 3:166–167.

Millhauser, G. L., E. E. Salpeter, and R. E. Oswald. 1988. Diffusion models of ion-channel gating and the origin of power-law distributions from single-channel recording. *Proc. Natl. Acad. Sci. USA.* 85: 1503–1507.

Montal, M., and P. Mueller. 1972. Formation of bimolecular membranes from lipid monolayers and study of their properties. *Proc. Natl. Acad. Sci. USA.* 65:3561–3566.

Nyquist, H. 1928. Thermal agitation of electric charge in conductors. *Phys. Rev.* 32:110–113.

Opsahl, L. R. 1933. Physical mechanisms of mechano-electrical transduction in the model channel forming peptide alamethicin. Ph.D. thesis. Cornell University, Ithaca, NY.

Petsko, G. A., and D. Ringe. 1984. Fluctuations in protein structure from x-ray diffraction. *Annu. Rev. Biophys. Bioeng.* 13:331–371.

Press, W. H., B. P. Flannery, S. A. Teukolsky, and W. T. Vetterling. 1987a. Numerical Recipes. Cambridge University Press, Cambridge. 381–454.

Press, W. H., B. P. Flannery, S. A. Teukolsky, and W. T. Vetterling. 1987b. Numerical Recipes. Cambridge University Press, Cambridge. 289–293.

Quinn, P. J. 1981. The fluidity of cell membranes and its regulation. *Prog. Biophys. Mol. Biol.* 38:1–104.

Rinehart, K. L., Jr., J. C. Cook, Jr., H. Meng, K. L. Olson, and R. C. Pandey. 1977. Mass spectrometric determination of molecular formulas for membrane-modifying antibiotics. *Nature.* 27:832–833.

Saffman, P. G. 1976. Brownian motion in thin sheets of viscous fluid. *J. Fluid Mech.* 73:593–602.

Saffman, P. G., and M. Delbrück. 1975. Brownian motion in biological membranes. *Proc. Natl. Acad. Sci. USA.* 72:3111–3113.

Sakmann, B., and E. Neher. 1983. Geometric parameters of pipettes and membrane patches. *In* Single-Channel Recording. E. Neher and B. Sakmann, editors. Plenum Press, New York and London. 37–51.

Sansom, M. S. P. 1991. The biophysics of peptide models of ion channels. *Prog. Biophys. Mol. Biol.* 55:139–235.

Sansom, M. S. P. 1993. Alamethicin and related peptaibols—model ion channels. *Eur. Biophys. J.* 22:105–124.

Schlessinger, J. 1986. Allosteric regulation of the epidermal growth factor receptor kinase. *J. Cell Biol.* 103:2067–2072.

Schottky, W. 1918. Über spontane Stromschwankungen in verschiedenen Elektrizitätsleitern. *Ann. Phys.* 57:541–567.

Schwarz, G., and P. Savko. 1982. Structural and dipolar properties of the voltage-dependent pore former alamethicin in octanol/dioxane. *Biophys. J.* 39:211–219.

Sigworth, F. J. 1983. Electronic design of the patch clamp. *In* Single-Channel Recording. E. Neher and B. Sakmann, editors. Plenum Press, New York and London. 3–35.

Sigworth, F. J. 1985. Open channel noise. I. Noise in acetylcholine receptor currents suggests conformational fluctuations. *Biophys. J.* 47:709–720.

Sigworth, F. J. 1986. Open channel noise. II. A test for coupling between current fluctuations and conformational transitions in the acetylcholine receptor. *Biophys. J.* 49:1041–1046.

Sigworth, F. J., and S. M. Sine. 1987. Data transformations for improved display and fitting of single-channel dwell time histogram. *Biophys. J.* 52:1047–1054.

Sigworth, F. J., D. W. Urry, and K. U. Prasad. 1987. Open channel noise. III. High-resolution recordings show rapid current fluctuations in gramicidin A and four chemical analogues. *Biophys. J.* 52:1055–1064.

Smythe, W. R. 1967. Static and Dynamic Electricity. McGraw-Hill, New York. 109–112.

Stevens, C. F. 1972. Inferences about membrane properties from electrical noise measurements. *Biophys. J.* 12:1028–1047.

Taylor, R. J., and R. de Levie. 1991. "Reversed" alamethicin conductance in lipid bilayers. *Biophys. J.* 59:873–879.

Unwin, P. N. T., and G. Zampighi. 1980. Structure of the junction between communicating cells. *Nature.* 283:545–549.

van der Ziel, A. 1970. Noise in solid state devices and lasers. *Proc. IEEE.* 58:1178–1206.

van Vliet, K. M., and J. R. Fassett. 1965. Fluctuations due to electronic transitions and transport in solids. *In* Fluctuation Phenomena in Solids. R. E. Burgess, editor. Academic Press, New York. 267–354.

Vogel, H. N. L., R. Rigler, S. Meder, G. Boheim, H.-H. Beck, W. Kurth, and G. Jung. 1993. Structural fluctuations between two conformational states of a transmembrane helical peptide are related to its channel-forming properties in planar lipid membranes. *Eur. J. Biochem.* 212: 305–313.

Voss, R. F., and J. Clarke. 1976. Flicker ($1/f$) noise: equilibrium temperature and resistance fluctuations. *Phys. Rev. B.* 13:556–573.

Woolley, G. A., and B. A. Wallace. 1992. Model ion channels: gramicidin and alamethicin. *J. Membr. Biol.* 129:109–136.